Environmental stress cracking and crazing in polymers in terms of irreversible thermodynamics

Hiroshi Okamoto and Yoshihito Ohde
Department of Engineering Sciences, Nagoya Institute of Technology, Gokisomachi, Shouwaku, Nagoya, 466, Japan
(*Received* 18 *June* 1981; *revised* 24 *October* 1981)

The processes in environmental stress cracking and crazing in polymers are analysed in terms of the irreversible thermodynamics. The thermodynamic potential of the system composed of the polymer matrix at a flaw tip region and its environmental liquid is constructed as a function of the concentration of the liquid migrated in the matrix and the dilative stress due to stress concentration. A state of the system is represented by a point in the thermodynamic potential diagram. The paths of the state shifts leading to failure in the diagram are governed by the shapes of the thermodynamic potential curves, the liquid concentrations giving the potentials a minimum, the critical concentration and the breakdown concentrations here introduced. Various kinetic data of environmental stress cracking in low density polyethylenes can be understood by the unified picture. The predictions of the theory are also consistent with the reported kinetic nature of crazing.

Keywords Mechanical behaviour; environmental stress cracking; crazing; polyethylene; irreversible thermodynamics; failure kinetics; crack growth

INTRODUCTION

In the presence of certain kinds of liquids, many polymeric materials undergo failute by brittle-like cracking and crazing by much loser mechanical load than would otherwise be necessary to cause failure. The failure by cracking is called environmental stress cracking (ESC).

Haward *et al.*[1] emphasized that the surface energy reduction effect by ESC active liquids plays an important role in collapsing voided structures in polyethylenes. Andrews *et al.*[2] also pointed out the importance of the effect in their study of environmental stress crazing in amorphous polymers above their glass temperatures. However, Gent[3] and Brown[4] derived relations between stress and swelling for crosslinked polymers and concluded that cracking and crazing are caused by the stress-induced swelling effect. Soni *et al.*[5] showed experimental evidence of stress-induced swelling in polyethylenes. A kinetic study based on the fracture mechanics of continuous bodies was developed by Williams *et al.*[6].

The growth rates of linear cracks in bent, low density polyethylene (LDPE) specimens immersed in ESC active liquids have been measured in our laboratory[7]. The Arrhenius plots of the growth rates exhibited various shapes. A thermodynamic analysis established in the course of the study has been successful in putting them in qualitative order. It may be applicable to the kinetics of brittle-like failures in other polymer–liquid pairs. Kambour's question[8] about the craze breakdown kinetics seems to be solved by it.

The concept of the stress-induced swelling is considered here but the main aim of this paper is in understanding the phenomena by irreversible thermodynamics. The fact that failure processes are irreversible has not been taken into account in previous theories. A preliminary study has already been carried out[9].

In the present experiments, the surface energy reduction and the hydrodynamic flow of liquids into polymer void structures[10,11] do not appear to be rate determining. The study of the microscopic structure and the stress field of polymer matrix around crazes or cracks has shown increasing progress[8,12–14].

THERMODYNAMIC PROCESSES

Environmental stress cracking and crazing

Consider the system representing the combination of the polymer matrix at a tip of a flaw or a crack in a specimen and its environmental liquid in an ESC experiment. When the specimen is loaded, the matrix is under intensified polyaxial stress induced by stress concentration.

The state of the system of a fixed size is defined by its temperature, stress and the concentration of the environmental liquid migrated into the matrix. When it is not in a thermodynamically stable state, it will shift to a more stable one where its thermodynamic potential descends. *Figure 1* shows the thermodynamic potential *versus* the liquid concentration curves.

The ESC growth processes are considered in this paper as the isothermal state shifts. The origin, O, in *Figure 1* corresponds to the state of the system at the beginning of an ESC experiment where a specimen has just beem immersed in a liquid but not yet loaded. After loading, stress concentrates in the polymer matrix of the system. The state of the system shifts to the point A by strain energy, then shifts towards the point M, the minimum of

0032-3861/82/081204-07$03.00

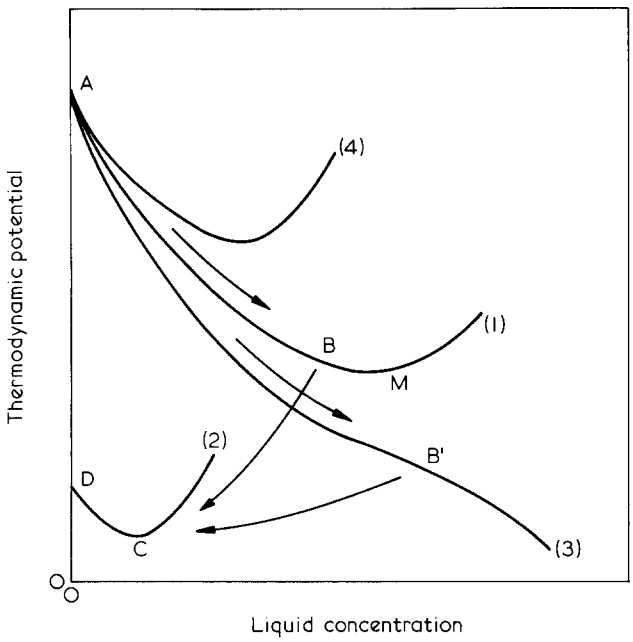

Figure 1 Thermodynamic potential diagram showing the processes in environmental stress cracking and crazing. The ordinate is the thermodynamic potential of the system composed of the polymer matrix at a flaw tip and its environmental liquid. The abscissa is the concentration of the liquid migrated in the polymer matrix. For labelling of points indicated in the Figure, see text

the thermodynamic potential (1) at that temperature and stress, by migration of the liquid molecules into the matrix. It is possible that the value of stress changes during the state shift, but this is ignored at present for simplicity. When the liquid concentration exceeds limit φ^* (breakdown concentration), the matrix breaks on account of the weakening induced by swelling. After breaking, the state is at point C, the minimum point of the thermodynamic potential (2) free from stress. The distance DO corresponds to the surface energy increment by breaking. The breakdown yields another stress concentrated region, and ESC grows through the repetition of the processes. The state departs from the curve (1) at the point B and shifts towards C. At the threshold of ESC growth, point B is near to M and may slightly exceed it to the right. The state shift beyond M must surmount the potential barrier and is very time consuming. In a steadily growing ESC, point B should be found between A and M. By elevation of temperature or increase in stress, the minimum and maximum of the potential merge into a point at the critical concentration φ_c and then vanish like curve (3). In this case, the restriction vanishes and the state can shift to an indefinitely dilute state. Another path to the breakdown A→B′→C′, an easier way to go to breakdown, must be proposed for the system. A sudden increase in the ESC growth rate may be observed. The point C′ representing the breakdown state is not the point C, if the path transition is induced by temperature elevation. But, for convenience in the diagram, the two points are not separated.

ESC will not occur when the concentration at M, φ_{min}, is less than φ^* by an amount (the curve (4)) or when the point C is above the point M. The state is then stabilized at M. To the naked eye the swelled state is seen as crazes. If lowering of the elastic modulus of the swelled region is enough, another stress concentrated region is produced and the craze will grow through repetition.

The ESC growth rate is determined as a net result of the consecutive processes. The shapes of the Arrhenius plots of PE ESC growth rates exhibited a great variety in appearance. This paper shows that the shapes and their polymer molecular weight dependence can be interpreted by the concept of the state shift in the diagram. Some of the reported craze kinetic data in amorphous polymers can be interpreted similarly.

FORMULATION BY A SIMPLE MODEL

To obtain the thermodynamic potential, the model shown in *Figure 2* is considered. The region I corresponds to the region at a crack (or a flaw) tip in a loaded polymer specimen and the region II to its environmental active liquid. The former consists of the matrix of n_r r-mers, i.e., polymer molecules and $n_{s,1}$ s-mers, i.e., liquid molecules and is subjected to a uniform polyaxial stress due to stress concentration, the mean principal stress of which is p_1. The latter consists of $n_{s,2}$ s-mers and subjected to a mean principal stress p_2 due to atmospheric pressure. The regions I and II are in contact and the s-mers can migrate between both phases; the total number of s-mers and the total volume being fixed and the system maintained at a temperature T. A fundamental assumption is that thermodynamic equilibrium is preserved within each region, but not between them. The thermodynamic potential of the system, G, is defined as the sum of the Gibbs free energy of each region:

$$G = n_r\mu_r + n_{s,1}\mu_{s,1} - p_1V_1 + n_{s,2}\mu_{s,2} - p_2V_2 \qquad (1)$$

where μ_r and $\mu_{s,1}$ are the Helmholtz chemical potentials of an r-mer and an s-mer in the region I respectively and $\mu_{s,2}$ is that of an s-mer in the region II and V_1 and V_2 are the volumes of the regions I and II respectively. The chemical potentials are conveniently approximated by the Flory–Huggins lattice theory. Designating the thermodynamic potential in its reduced form $G/(kTrn_r)$ $\tilde{G}$, we obtain:

$$\tilde{G} = (1/r)\ln(1-\varphi) + (1/s)(\varphi\ln\varphi)(1-\varphi) + \chi\varphi - \Delta p\varphi/(1-\varphi) + \text{constant} \qquad (2)$$

where φ is $sn_{s,1}/(rn_r + sn_{s,1})$, the volume fraction of the s-

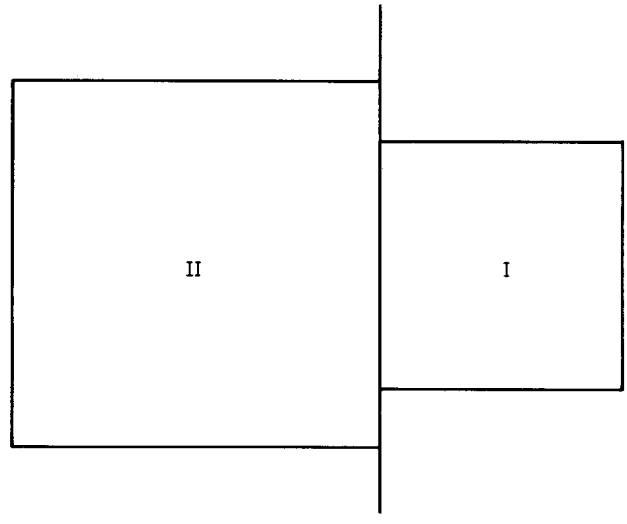

Figure 2 Model representing the regions in which ESC occurs. Region I corresponds to the region just at a flaw tip in a loaded polymer specimen and the region II to its environmental liquid

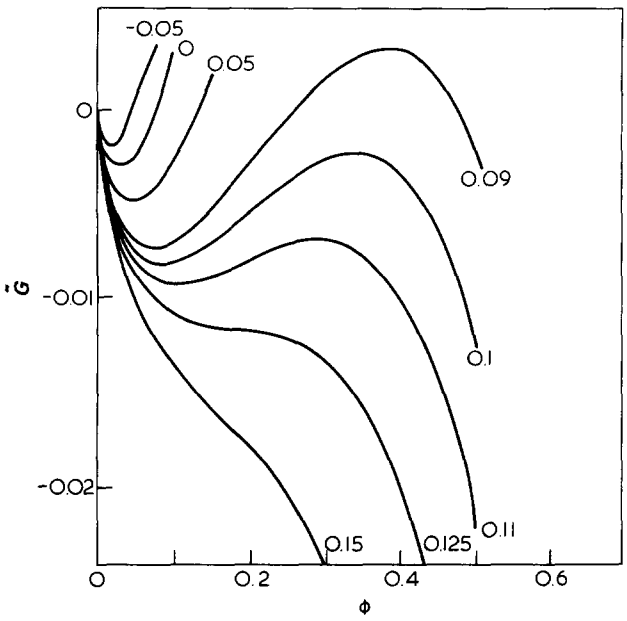

Figure 3 Reduced thermodynamic potential $\tilde{G}$ *versus* liquid concentration ϕ. The parameters are, r = 1000, s = 8, χ = 0.35. The values of Δp are indicated in the Figure

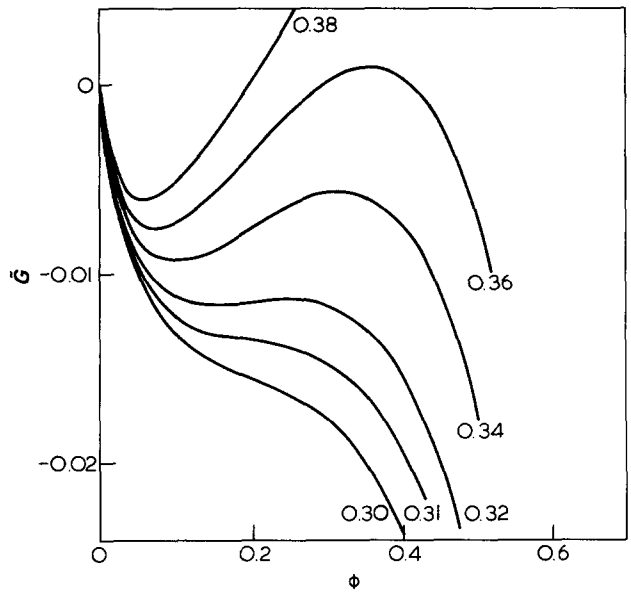

Figure 4 Reduced thermodynamic potential $\tilde{G}$ *versus* liquid concentration ϕ. The parameters are r = 1000, s = 8, Δp = 0.1. The values of χ are indicated in the Figure

mers in the region I, χ is the interaction parameter inversely proportional to T, defined for a pair of an r-mer segment and an s-mer segment and Δp is $(p_1 - p_2)/kT$ (the segment volume being 1).

Figure 3 shows the curves $\tilde{G}$ *versus* φ of the system with $r = 1000$, $s = 8$, $\chi = 0.35$ and a variety of Δp values. The system simulates the pair of an LDPE and a nonionic surfactant NS210. (See the next section.) When Δp is negative or zero, φ_{min} is close to 0, i.e., the pair is almost imcompatible. For a positive Δp, $\tilde{G}$ exhibits a minimum and a maximum. With the increase in Δp, φ_{min} increases. When Δp equals a value, Δp^*, φ_{min} equals φ^*. ESC will start to grow at a Δp slightly less than Δp^*. With a further increase in Δp, $\tilde{G}$ becomes monotonic decreasing. *Figure 4* shows the $\tilde{G}$ curves of the same system calculated for a fixed Δp and a variety of χ values. (As to the parameter values, see the next section.) It shows that φ_{min} will exceed φ^* for χ values smaller than a value χ^*. *Figure 5* shows those of the system simulating the pair of an LDPE and propanol for a fixed Δp and a variety of χ values. (See the next section.)

The potential curves are not greatly affected by polymer molecular weights and curves calculated by $r = 100$ cannot be separate in the figures. It is natural to suppose that φ^* is changed by polymer molecular weights so that the higher the molecular weights, the larger the values of φ^*.

The rate of the state shift from A to B is governed by the gradients of the thermodynamic potential. Let $f(i,t)$ be the probability that there are i s-mers in the region I at a time t. Then:

$$\partial f(i,t)/\partial t = [f(i+1,t)\Lambda_{i+1,i} - f(i,t)\Lambda_{i,i+1}] - [f(i,t)\Lambda_{i,i-1} - f(i-1,t)\Lambda_{i-1,i}] \quad (3)$$

where $\Lambda_{i,i\pm1}$ means the probability that an s-mer migrate in (+sign) or out from (−sign) the region I with i s-mers in a unit time interval. According to the Eyring's rate theory, $\Lambda_{i,i\pm1}$ may be written by:

$$\Lambda_{i,i\pm1} = \Lambda_0 \exp[-(\Delta h_{i,i\pm1} + (1/2)\Delta G^{\pm}(i))/kT] \quad (4)$$

where:

$$\Delta G^{+}(i) = G(i+1) - G(i),$$

$$\Delta G^{-}(i) = G(i-1) - G(i)$$

Λ_0 is a constant, weakly dependent on temperature, and $\Delta h_{i,i\pm1}$ is the activation energy measured from the mean level of the thermodynamic potentials of the two states with i and $i \pm 1$ s-mers. To simplify the situation, $\Delta h_{i,i\pm1}$ is assumed constant, Δh, irrespective of i hereafter. The mean time of the state shift A to B, $\langle\tau\rangle$, is given through

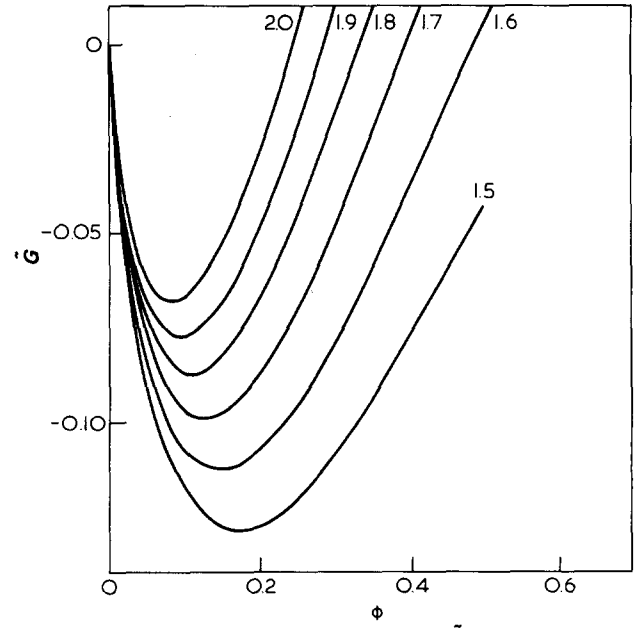

Figure 5 Reduced thermodynamic potential $\tilde{G}$ *versus* liquid concentration ϕ. The parameters are r = 1000, s = 1, Δp = 0.1. The values of χ are indicated in the Figure

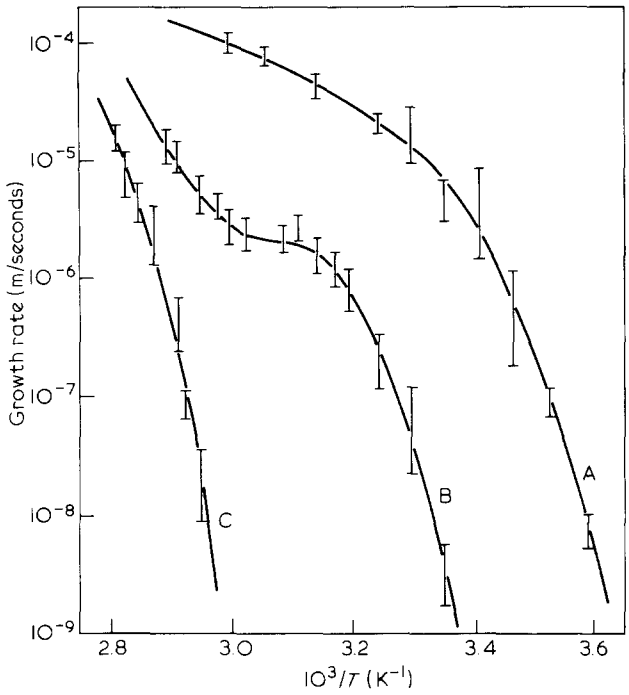

Figure 6 Growth rates v of PE A, B and C ESC induced by NS210 *versus* reciprocal temperature $1/T$

solving the difference equation (3) with respect to $f(i,t)$ under the initial condition

$$f(i,0)=\delta(i) \tag{5-1}$$

and the boundary conditions at $i=0$

$$\partial f(0,t)/\partial t = f(1,t)\Lambda_{1,0} - f(0,t)\Lambda_{0,1} \tag{5-2}$$

and at $i=i^*$

$$f(i^*,t)=0 \tag{5-3}$$

where i^* is the number of the s-mers in the region I at the point B. A convenient time t_0, $t_0=\Lambda_0\exp[-\Delta h/kT]\cdot t$ is introduced. The mean time of shift A to B is given by:

$$\langle\tau\rangle=\langle\tau_0\rangle\Lambda_0^{-1}\exp[\Delta h/kT] \tag{6}$$

where $\langle\tau_0\rangle$ is given by:

$$\langle\tau_0\rangle=\exp[\Delta G^+(i^*-1)/2kT]\int_0^\infty t_0 f(i^*-1,t_0)\mathrm{d}t_0 \tag{7}$$

If the contribution of the time necessary for the state shift B to C is small, ESC growth rate v is inversely proportional to $\langle\tau_0\rangle$

$$v\propto\langle\tau_0\rangle^{-1}\Lambda_0\exp[-\Delta h/kT]. \tag{8}$$

As will be described in the next section, the dependence of $\langle\tau_0\rangle$ on temperature is often so large that the slopes of the Arrhenius plots of growth rates do not always give the activation energy Δh.

COMPARISON WITH EXPERIMENTS

General

The fact that ESC is a brittle-like failure and that ESC active liquids are non-solvents for polymers are consistent with the present picture. That the region in a specimen satisfying the condition $\Delta p \geqslant \Delta p^*$ is a very limited one at a flaw or a crack tip makes the ESC nature apparently brittle-like. These points were explained by the previous theories[3,4]. The interpretation of kinetic data in the present theory is new.

Shapes of the Arrhenius plots of ESC growth rates found in LDPE

Various experimental data of LDPE ESC growth have been accumulated in our laboratory. The active liquids used have covered pure and aqueous solutions of several non-ionic surfactants and n-alcohols, ethers derived from diethylene glycol, poly-methylphenylsiloxane and poly-dimethylsiloxane (PDMS) of various molecular weights. The data and the discussion will appear fully in consecutive papers. Examples are shown in *Figures 6*, *7* and *8*. Three LDPE's, A, B and C with different molecular weights, were used. (See *Table 1*.) The measurements of ESC growth rates were similar to those reported[7], in which single cracks growing along the ridges of bent specimens were pursued. A little modification in the procedure will be described in a following paper.

Figure 6 shows the Arrhenius plots of the growth rates obtained by using NS210 as an active liquid and *Figure 7* shows those obtained by NS215. For NS210 and NS215, see *Table 2*. The figures show that the shapes of the Arrhenius plots roughly consist of three ranges. In the low temperature range, there was a very sharp increase in the growth rates by a slight elevation of temperature. A relaxation of the growth rate increase followed it in the medium temperature range. At the high temperature range, the growth rates again increased rapidly. Typical

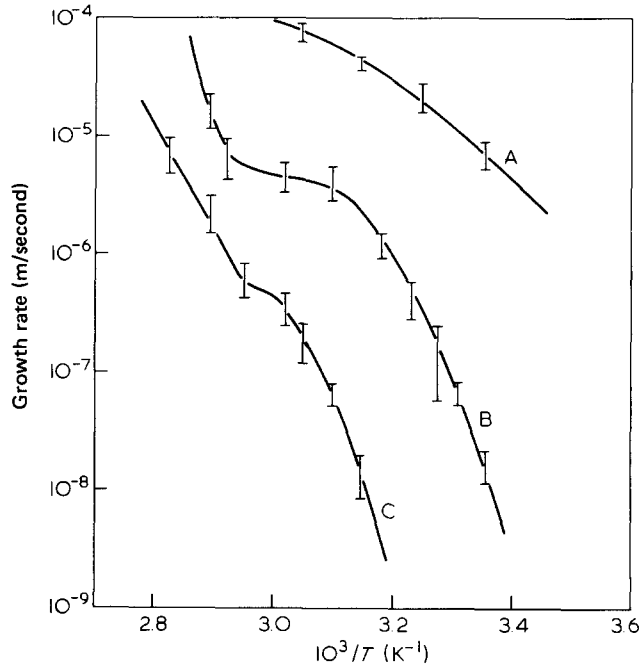

Figure 7 Growth rates v of PE A, B and C ESC induced by NS215 *versus* reciprocal temperature $1/T$

behaviours were exhibited in the plots of PE B ESC induced by the both liquids. In the plots of PE A ESC, the high temperature behaviour seemed to be outside the measurable range. The plots of PE C ESC induced by NS210 exhibited only the high temperature behaviour but those by NS215 exhibited the three behaviours. The sizes of the medium temperature ranges were influenced by polymer molecular weight in that the higher the molecular weights, the narrower the ranges. The dependence of the growth rates on polymer molecular weights in the low temperature range was marked. *Figure 6* shows that the growth rates in that region differed over two decades between PE A and B, molecular weights of which were 35 000 and 42 000 respectively. The growth was suppressed at the same temperature by PE C, having molecular weight 55 000. The dependence of the growth rates on polymer molecular weights was moderate in the medium temperature range and was likely to be similar in the high temperature range. The growth rate behaviours like these exhibited by PE ESC induced by the other liquids such as PDMS's excepting low molecular weight ones. The active liquids having larger molecular sizes and smaller interaction parameter values are those of the liquids belonging to this group.

Figure 8 shows those obtained by propanol. All plots were roughly linear and exhibited strong temperature dependence. The dependence of the growth rates on polymer molecular weights was marked. The growth rate behaviours like these were exhibited by other liquids such as alcohols and low molecular weight non-solvents. The active liquids having smaller molecular sizes and larger interaction parameter values are those of the liquids belonging to this group.

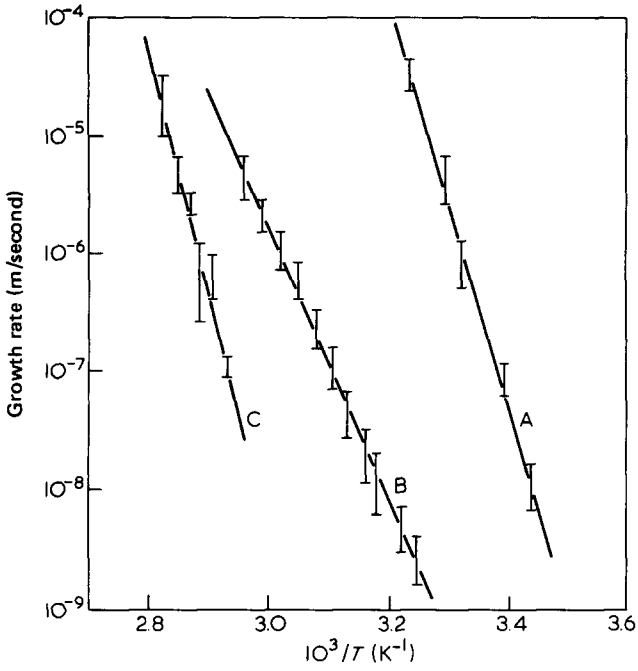

Figure 8 Growth rates v of PE A, B and C ESC induced by propanol *versus* reciprocal temperature $1/T$

The boundary between the two groups was not strict. It was affected by the amount of the applied load. The true situation will be discussed shortly.

As mentioned before, the thermodynamic potentials in *Figures 4* and *5* are those of the systems simulating the pair of an LDPE and NS210 and those corresponding to an LDPE and propanol pair respectively. The former are conceived as the representatives of the thermodynamic potentials of the pairs of polymers and first group liquids. The latter are those of the pairs of polymers and second group liquids. The ranges of the interaction parameter values were roughly estimated so as to cover the experimental temperature ranges by using the formula $\chi=(\delta_p-\delta_l)^2V_0/RT$. The solubility parameters of a polymer and a liquid, δ_p and δ_l, were estimated by following the method of Small and Hoy[16]. The segment molar volume V_0 was assumed to be that of propanol. The value of Δp, 0.1, is estimated from an assumption that $\Delta p=(\sigma_y/3RT)V_0$, where σ_y is the yield strength of the polymer at a room temperature. The variation of Δp with temperature was excluded for simplicity. The estimation of Δp values may be controversial and will be touched again in the next section. *Figure 4* shows that in the range examined there is a critical value of χ, χ_c, (or a critical temperature T_c) below (or above) which the potential curves are monotonic decreasing. Contrary to this, each curve in *Figure 5* has a minimum. The critical value of χ of the pair is 1.1 which is outside the experimental temperature range.

Firstly we consider the low and the medium temperature behaviours found in the experiments by inspecting the thermodynamic potentials in *Figure 4*. By elevation of temperature or decreasing the interaction parameter values, ESC will start to grow at a temperature where χ is close to χ^*. The slopes of the growth rate Arrhenius plots are expected to be greatest there. Slight

Table 2 List of surfactants

Commercial name	Rational formula
NS210*	$C_9H_{19}C_6H_4O(CH_2CH_2O)_{10}H$
NS215*	$C_9H_{19}C_6H_4O(CH_2CH_2O)_{15}H$

* Manufactured by Nippon Oil & Fats Co. NS210 is nearly the same material known as Igepal CO630 or Antarox CO630

Table 1 Specification of polyethylene

Polyethylene*	Melt index (10^{-5} kg s^{-1})	Density (10^3 kg m^{-3})	Yield strength (MN m^{-2})	Molecular weight†
A	3.33	0.918	8.8	32000
B	0.67	0.920	10.8	45000
C	0.17	0.920	10.8	55000

* Manufactured by Mitsubishi Petrochemical Co.

† Molecular weights were estimated through viscosity measurements of *p*-xylene solutions at 354 K by using the relation[15], $[\eta]$ (dl g^{-1}) $0.105 \times 10^{-2} M^{0.63}$

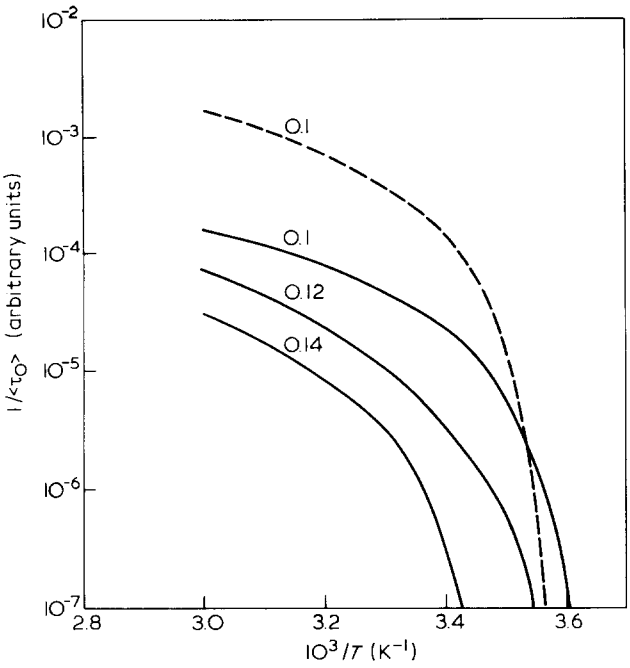

Figure 9 Reciprocal of mean time of state shift A to B, $1/\langle\tau_0\rangle$, *versus* reciprocal temperature $1/T$. Calculations were performed for the two systems, the thermodynamic potentials of which were depicted in *Figures 4* and *5*. The solid line curves were calculated for the former. The dotted line curves were for the latter. The parameters are, $r = 100$, $n_r = 22$ and the values of ϕ^* are indicated in the Figure. For fuller accounts, see the text

differences in the values of φ^* due to polymer molecular weight differences can lead to extraordinary differences in the growth rates.

Numerical calculations of $\langle\tau_0\rangle$ were performed to confirm the expectation by using equation (7). The solid curves in *Figure 9* show the relations $1/\langle\tau_0\rangle$ *versus* $1/T$ of the system simulating the LDPE and NS210 pair obtained by the simplification that φ^* is held constant irrespective of temperature. The conversion of χ to $1/T$ was adjusted so that the ESC starting temperature estimated by putting $\varphi^* = 0.1$ is near to that of PE A ESC found in the experiments. The curves confirm the expectation. Further, the relaxation of the growth rate increase is exhibited in the medium temperature range. The growth rate differences by values of φ^*, or by polymer molecular weights, are diminished in that range. These agree with the experiments found in the LDPE and the first group liquid pairs. Compare the solid curve ($\varphi^* = 0.1$) with the dashed curve in *Figure 9* which was calculated for the system simulating the LDPE and propanol pairs ($\varphi^* = 0.1$). The growth rate increase shows less relaxation in the latter curve. The difference in the values of the factor $\Lambda_0 \exp[-\Delta h/kT]$ between the two is discarded because our interest is only in the shapes of the curves. The calculated growth rate increase with temperature elevation and with the decrease in φ^* may appear too small compared to the experiments. No relaxation of the growth rate was found in the experiments of the LDPE and propanol pairs. The numerical calculations were performed for the systems having a size of rn_r, 2 200, which is probably too small compared to a real one. Increasing the value of rn_r will make the calculated ones more like the experimental.

The sudden increase in the growth rates in the high temperature range found in the LDPE and first group liquid pairs can be attributed to the vanishing of the potential minimum above the temperature T_c shown in *Figure 4*. At that temperature, another path of the state shift to the breakdown (A→B′→C′) which is easier to go to the breakdown state is released. The sudden increase in the growth rate occurs in the course of the path transition. The reason why the high temperature behaviours were not observed by PE ESC induced by the second group liquids is now obvious. It is because their critical temperatures are outside the experimental ranges.

After the transition, a relaxation of the growth rate increase or a steady growth region will follow. But it seemed to be outside the experimental ranges for these examples. In recent examples using PDMS's as active liquids, we found a few examples which seemed to show it.

For higher molecular weight polymers, the value of φ^* may exceed that of φ_c. The path transition in this case being absent, the state shift goes along A→B′→C′ from the beginning and the low and the medium temperature behaviours will not be observed. The ESC in PE C induced by NS210 is an example (*Figure 6*).

Experiments in craze breakdown kinetics

According to Rudd[17], the breakdown time of loaded polystyrene immersed in t-butylalcohol increased with the eleventh power of polymer molecular weight. Kambour[8] stated in his review of crazing that the threshold strain for craze initiation differs little with increasing polymer molecular weights but the ease of craze breakdown differs greatly as revealed by Rudd. Kambour added that the chain entanglement concept, therefore, cannot be unaltered to the breakdown mechanism of the crazes. The proposed picture qualitatively reproduced the peculiar kinetic properties to crazing. Since the thermodynamic potentials are, and the liquid concentrations at the observable stable swelled states will be, differed only slightly by polymer molecular weights, the stress or its equivalent strain necessary for yielding crazes will not be affected by polymer molecular weights. The breakdown time, if the breakdown concentrations are close to φ_{min}, will be greatly differed by polymer molecular weights as seen in the last subsection. The chain entanglement will play its role through the value of φ^*.

DISCUSSION

We have confined our attention to the shapes of the thermodynamic potential curves and the values of φ^* relative to those of φ_{min} and φ_c. They govern the paths of the state shift from A to C or C′ (*Figure 1*). The shapes of the Arrhenius plots of the ESC growth rates and their molecular weight dependences in LDPE's are consistently understood in terms of that concept. In the present case, the slopes of the Arrhenius plots do not give the activation energy for the molecular transport (in the steadily growing region, there may be exceptions). The kinetic properties peculiar to crazing and craze breakdown are reasonably understood in a similar way. The essentials of the ESC kinetics are certainly included in the proposition. The success remains qualitative and the quantitative approach is outside the scope of this study.

The contribution of the surface energy DO in *Figure 1*, if any, seems not to play a rate determining role in the present experiments. There was also no sign that the flow of liquids determines the rates.

The formulation of the thermodynamic potential was made by a very simple model to overcome the otherwise inaccessible complexity involved in the actual processes. The molecular orientation and the polymer crystallinity which will play some role in the processes are excluded from the model. In the numerical calculations of the last section, the values of Δp were assumed constant in the experimental temperature ranges. The definition of Δp indicates it will not. Separate numerical calculations told us that to vary Δp proportionally to $1/T$ brought no change in our discussion. Our choice of the Δp values was arbitrary but not too far from the true situation. The values of χ were evaluated in the generally accepted way, but this is not always reliable for the incompatible liquid pairs[18]. The success of our treatment tells us that the ambiguities are of minor importance and may be in part mutually cancelling in the determination of the shapes of the Arrhenius plots.

There may be room to improve the thermodynamic potential formulation and the breakdown criterion by refinement of the model. The improvement, if attained, will give a more detailed understanding of the ESC growth processes. Even in that case, the concept of the path of the state shift will give a basic guide for the study.

A straightforward extension of the theory to the cases in which the active liquids are mixtures was made. A preliminary study based on it was successful in predicting the qualitative behaviours of the growth rates *versus* the liquid compositions. It supports our thermodynamic approach in a different way.

Equation (2) showed the polymer matrix in the region I to be a simple assembly of molecules. Its replacement by a rubbery network as in the previous theories[3,4] essentially introduces no change in the present discussion.

ACKNOWLEDGEMENTS

The authors are grateful to Mitsubishi Petrochemical Co. and Nippon Oil and Fats Co. for their presentation of materials. The authors thank Dr M. Sugiyama for his discussion during the work and Mr Y. Nagata for his help in the experimental work. Part of the study was supported by the Grant-in-Aid for Developmental Scientific Research presented by the Japanese Ministry of Education, Science and Culture in 1980.

REFERENCES

1 Haward, R. N. and Owen, D. R. J. *Proc. Roy. Soc. London (A)* 1978, **352**, 265
2 Andrews, E. H. and Bevan, L. *Polymer* 1972, **13**, 337
3 Gent, A. N. *J. Mater. Sci.* 1970, **5**, 925
4 Brown, H. R. *Polymer* 1978, **19**, 1186
5 Soni, P. L. and Geil, P. H. *J. Appl. Polym. Sci.* 1979, **23**, 1167
6 Williams, J. G. and Marshall, G. P. *Proc. Roy. Soc. London (A)* 1975, **342**, 20
7 Ohde, Y. and Okamoto, H. *J. Mater. Sci.* 1980, **15**, 1539
8 Kambour, R. P. *J. Polym. Sci. Macromol. Rev.* 1973, **7**, 1
9 Okamoto, H. and Ohde, Y. *Polymer* 1980, **21**, 859
10 Shanahan, M. E. R. and Schultz, J. *J. Polym. Sci., Polym. Phys. Edn.* 1976, **14**, 1567
11 Bubeck, R. A. *Polymer* 1981, **22**, 682
12 Isaksen, R. A., Newman, S. and Clark, R. J. *J. Appl. Polym. Sci.* 1963, **7**, 515
13 Bandyopadhyay, S. and Brown, H. R. *Polymer* 1978, **19**, 589
14 E.g., Lauterwasser, B. D. and Kramer, E. J. *Phil. Mag. A* 1979, **39**, 469
15 Trementozzi, Q. A. *J. Polym. Sci.* 1957, **23**, 887
16 Burrell, H. 'Polymer Handbook' (Eds. J. Brandrup and E. H. Immergut), John Wiley and Sons, New York, 1975, Ch. IV–15
17 Rudd, J. F. *J. Polym. Sci. B* 1963, **1**, 1
18 E.g., Konningsveld, R. and Kleintjens, L. A. *J. Polym. Sci. A-2* 1970, **8**, 1261